

Correlation between dielectric constant and chemical structure of sodium silicate glasses

C. H. Hsieh and H. Jain^{a)}

Department of Materials Science and Engineering, 5 East Packer Avenue, Lehigh University, Bethlehem, Pennsylvania 18015

E. I. Kamitsos

Theoretical and Physical Chemistry Institute, National Hellenic Research Foundation, 48 Vass. Constantinou Avenue, Athens 116 35, Greece

(Received 18 September 1995; accepted for publication 30 April 1996)

The chemical structure of sodium aluminosilicate glasses is determined by high resolution x-ray photoelectron spectroscopy (XPS) as silicon is gradually replaced by aluminum. A well-defined chemical state is found for silicon, aluminum, and sodium atoms, while three different environments are identified for oxygen atoms corresponding to Si–O–Si, Si–O–Al, and Si–O–Na bonds. The binding energy of Na 1s photoelectrons increases significantly with increasing aluminum substitution while that of Al 2p and components of O 1s photoelectrons remains approximately constant. Thus, the ionicity of sodium increases with aluminum amount, but the overall electron density around silicon, aluminum, and different types of oxygen atoms remains unchanged. The dielectric constant of the glasses increases with increasing aluminum substitution. It is analyzed in terms of the polarizabilities of constituent structural units, *viz.*, silicon tetrahedra, nonbridging oxygen–sodium ion pairs, and aluminum tetrahedron–sodium ion pairs. The electronic polarizability of oxygen ions depends linearly on their negative charge and can be correlated to the O 1s XPS binding energy. The ionic polarizability of sodium ions increases with an increasing aluminum amount, and correlates directly with the Na 1s XPS binding energy. © 1996 American Institute of Physics. [S0021-8979(96)06015-X]

I. INTRODUCTION

Dielectric constant is a property of glass which is particularly important for many applications in electronics. For example, glass with low dielectric constant (<10) is a crucial element of high-performance microelectronic systems. It is used as a substrate or a passivation and dielectric layer in semiconductor packaging,^{1–3} and in thick film resistors.⁴ Glasses for such applications include silica and borosilicate- and cordierite-based compositions.^{2,5,6} On the other hand, a glass with high dielectric constant is desirable for applications such as high energy capacitors⁷ and multilayer dielectrics.⁴ Typically, high dielectric constant glasses contain heavy-metal cations like Pb, Ba, Bi, and W.⁷

To tailor the dielectric constant of glass for a certain application, it is important to understand the mechanism of dielectric polarization which arises from the constituent species including ions, ion pairs, and other building units of the structure. Typically the dielectric constant is analyzed in terms of the polarizability of the ions or structural units. For example, Kenmuir *et al.*⁸ have studied Mg–Al–Si oxynitride glasses and found that the addition of nitrogen increases the dielectric constant. Singer and Tomozawa⁵ have found for cordierite-based oxyfluoride glasses that fluorine substitution results in a lower dielectric constant. They conclude that, along with the reduced number of polarizable ions per unit volume, the lower polarizability of fluorine than that of oxygen ions reduces the dielectric constant. For the PbO–B₂O₃–SiO₂–GeO₂ glasses, Kobayashi³ has suggested

that the substitution of highly polarizable Pb²⁺ ions by less polarizable B³⁺ or Si⁴⁺ ions decreases the overall polarizability and increases the stability of glasses. Hampton *et al.*⁹ and El-Mallawany¹⁰ have explained the dielectric constant of pure and binary tellurite glasses by considering the polarizability of TeO₂ and WO₃ units. They report that the polarizability is higher for a TeO₂ than a TeO₂–WO₃ unit. Sidek *et al.*¹¹ have found for the samarium phosphate glasses that Sm₂O₃ does not alter the polarizability at low concentrations and that the dielectric constant is determined by the P₂O₅ polarizability. Often, the polarizability has been considered independent of composition. For example, in the study of cordierite-based oxyfluoride glasses,⁵ the same value of polarizability has been assigned for oxygen and fluorine ions independent of composition. On the other hand, sometimes the polarizability is considered to be dependent on composition, such as, in the study of pure and binary tellurite glasses,¹⁰ where the decrease of polarizability from TeO₂ to TeO₂–WO₃ units is explained by the increase in Te–O and W–O bond energies.

In general, one expects that the polarizability of ions and structural units would depend on the charge and bond strength of the polarizable species. However, to the best of our knowledge an explicit correlation between the dielectric constant and chemical structure has never been established. In our previous study of the structure of sodium aluminosilicate (SAS) glasses by x-ray photoelectron spectroscopy (XPS),¹² it was found that sodium ions are only partially ionized in sodium trisilicate glass and their ionicity increases when silicon is substituted by aluminum. The physical structure of the glass remains essentially unaffected because the

^{a)} Author to whom correspondence should be addressed; Electronic mail: hj00@lehigh.edu

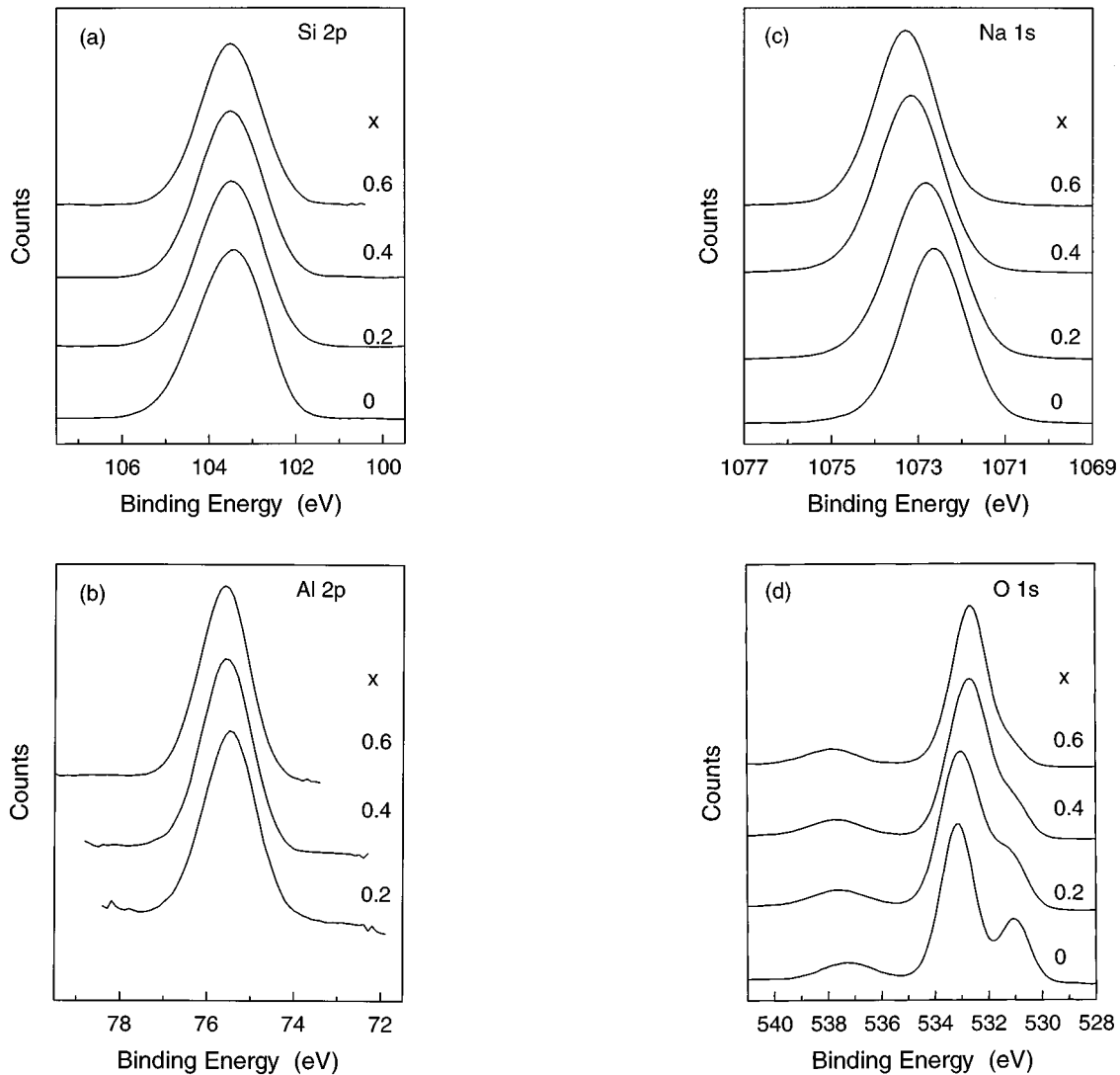


FIG. 1. X-ray photoelectron spectra of (a) Si $2p$, (b) Al $2p$, (c) Na $1s$, and (d) O $1s$ for the SAS glasses.

basic building block of the structure, SiO_4 tetrahedron, is simply replaced by an AlO_4 tetrahedron without appreciably affecting the molar volume. These observations offer a model example for understanding how the redistribution of electrons and a change of chemical structure can affect the dielectric constant of glasses. Thus, the purpose of this article is: first, to present additional details of XPS for understanding all the bonding changes in the structure of sodium aluminosilicate glass; second, to investigate the polarizability of ions or structural units; and finally, to discuss the correlation between dielectric constant and chemical structure.

II. EXPERIMENT

A. Sample preparation

The glasses were prepared according to the formula $\text{Na}_2\text{O} x\text{Al}_2\text{O}_3(3-2x)\text{SiO}_2$ where $x=0, 0.2, 0.4,$ and 0.6 . This composition series emphasizes the substitution of silicon by aluminum so that the ratio of the concentration of network modifier (Na) to network former (Si+Al) cations remained constant. The glasses were made from reagent grade

Na_2CO_3 , Al_2O_3 , and SiO_2 by conventional melt-quench method. The annealed glass samples were homogeneous and showed no stress when viewed with polarized light. The samples were cut to 1 mm thickness for further experiments. For details of glass preparation, the reader is referred to Ref. 12.

B. X-ray photoelectron spectroscopy

The Si $2p$, Na $1s$, O $1s$, and Al $2p$ x-ray photoelectron spectra were obtained using a high resolution Scienta ESCA-300 spectrometer. The instrument was operated in a mode that yielded a Fermi level width of 0.4 eV for silver. At this level of resolution, the instrumental contribution to the line width was extremely small. The spectra were taken on a freshly created sample surface obtained by fracturing it *in situ* inside the high vacuum chamber. The sample surface was flooded with a beam of low energy electrons to minimize the surface charging. Further details of the experiment are given elsewhere.¹²

C. Dielectric constant measurement

The dielectric constant was measured using a General Radio 1621 capacitance measurement system which utilizes a Wheatstone-type capacitance bridge with transformer ratio arms. Gold electrodes with a three-terminal configuration were applied to the sample surfaces by vacuum evaporation. The sample was placed in a tube furnace, and the temperature was monitored by a thermocouple which almost touched the sample. The sample cell and all leads were surrounded by a shield connected to ground to avoid electromagnetic interference. The ac capacitance C and conductance G , of the samples were determined by balancing the capacitance bridge in the frequency f range of 10 Hz–100 kHz at room temperature. Dielectric constant, $\epsilon(f)$, was calculated from capacitance by multiplying with an appropriate geometric factor.

D. Density measurement

The density was measured at room temperature using the Archimedes method with deionized water with an error <0.1%.

III. RESULTS

A. X-ray photoelectron spectroscopy

The photoelectron spectra for Si $2p$, Al $2p$, and Na $1s$ electrons show a symmetric single peak for the present SAS glasses [Figs. 1(a)–1(c)]. The spectra for O $1s$ electrons, however, reveal in Fig. 1(d) a second peak at the lower binding energy side of the main peak for sodium trisilicate glass, which becomes gradually smaller, ultimately appearing as a shoulder of the main peak when the substitution by Al increases. This result was explained by considering the presence of three distinct types of oxygen atoms in Si–O–Si, Si–O–Al, and Si–O–Na bonds.¹² Here the O $1s$ spectra are decomposed into three components by first choosing the relative charge density of various types of oxygen as a guide for the initial binding energies for the three components. The computer program then determines the best fitted parameters with the constraint that the peak positions remain within ± 0.5 eV. Under these conditions, the error bar is ~ 0.1 eV for the various oxygen peaks, which is the same as the experimental error. For evaluating the various spectra, the Si $2p$ peak at 103.5 eV is chosen as the most appropriate internal binding energy reference because the chemical environment of silicon remains essentially unaffected by aluminum substitution.¹² The binding energies of Na $1s$, Al $2p$, and O $1s$ peaks for the three types of oxygen ions are reported in Table I. It can be seen from Table I that, while the binding energies of Al $2p$ and O $1s$ electrons do not change significantly, the binding energy of Na $1s$ electrons increases by ~ 0.7 eV from sodium trisilicate glass to the glass containing the largest amount of aluminum.

B. Dielectric constant

The measured dielectric constants of the four glasses at 25 ± 0.7 °C are reported as a function of frequency in Fig. 2. It shows that the dielectric constant decreases for each glass

TABLE I. Binding energy (eV) of Na $1s$, O $1s$, and Al $2p$ electrons of the SAS glasses.

Al/Na	Na $1s$	O $1s$			Al $2p$
		Si–O–Si	Si–O–Al	Si–O–Na	
0	1072.6(4)	533.1	...	531.0	...
0.2	1072.8(5)	533.2	532.6	531.2	75.5
0.4	1073.1(9)	533.2	532.5	531.1	75.6
0.6	1073.3(1)	533.5	532.6	531.3	75.6

when the frequency increases. To obtain the dielectric constant that arises only from the electronic and ionic polarizations, the data are analyzed using Cole–Cole plot for complex dielectric constant $\epsilon^* = \epsilon' - i\epsilon''$, where ϵ' is the real part, and ϵ'' is the imaginary part of the dielectric constant. ϵ' is equal to the measured ϵ , and $\epsilon'' = \sigma/\omega\epsilon_0$ where σ is the conductivity, ω is the angular frequency, and ϵ_0 is the vacuum permittivity. A Cole–Cole plot is a complex dielectric constant plot with ϵ' on the x -axis and ϵ'' on the y -axis to show the dielectric relaxation behavior of a material. It is known empirically¹³ that the conductivity of glass follows a power law at high frequencies: $\sigma = \sigma_{dc} + A\omega^s$, where σ_{dc} is the frequency independent dc conductivity, and A and s ($0 < s < 1$) are fitting parameters. We identify the frequency dependent component of total conductivity with $\sigma_{ac} \approx A\omega^s$. Therefore, one has $\epsilon'' = \epsilon''_{dc} + \epsilon''_{ac}$, where $\epsilon''_{dc} = \sigma_{dc}/\omega\epsilon_0$ and $\epsilon''_{ac} = \sigma_{ac}/\omega\epsilon_0 = A/\omega^{1-s}\epsilon_0$. Since a Cole–Cole plot is to represent the dielectric relaxation, ϵ''_{ac} is used in the plot. According to the Kramers–Kronig transformation which relates ϵ' and ϵ''_{ac} at the high frequency end, the Cole–Cole plot becomes a straight line inclined at an angle $(1-s)\pi/2$ to the real axis,¹³ as shown in Fig. 3 for the SAS glasses. Here σ_{ac} was calculated by subtracting σ_{dc} from the measured σ ; σ_{dc} itself was determined by the complex impedance analysis.¹⁴ The dielectric constant obtained by extrapolating each line to the real axis is shown in Fig. 4. It is called the intermediate-

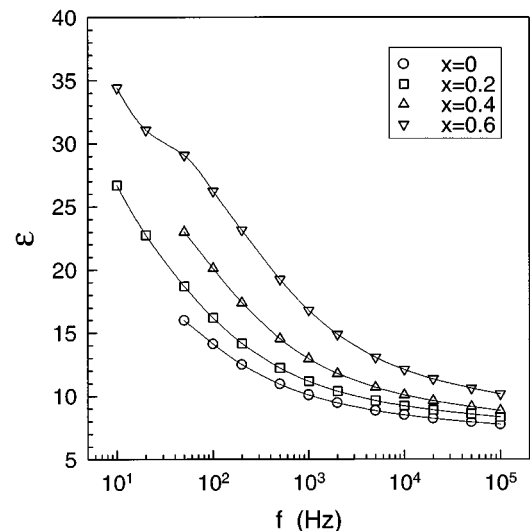


FIG. 2. Frequency dependence of the dielectric constant of the SAS glasses at 25 °C.

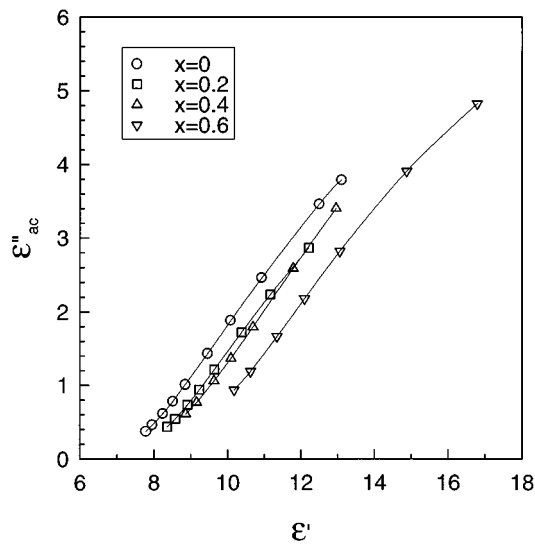


FIG. 3. Cole-Cole plots of the SAS glasses at 25 °C.

frequency dielectric constant $\epsilon_{i.f.}$ to distinguish it from the optical-frequency dielectric constant ϵ_{∞} which usually stands for the dielectric constant from electronic polarization only. It can be seen from Fig. 4 that $\epsilon_{i.f.}$ increases with the aluminum content in the glass.

C. Density

The composition dependence of the measured densities is shown in Fig. 5. It shows that the density increases monotonically with an increasing amount of Al substitution in the SAS glasses.

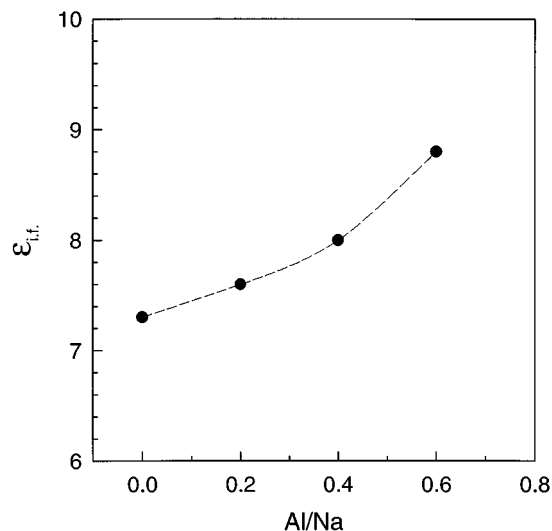


FIG. 4. Intermediate-frequency dielectric constant of the SAS glasses at 25 °C.

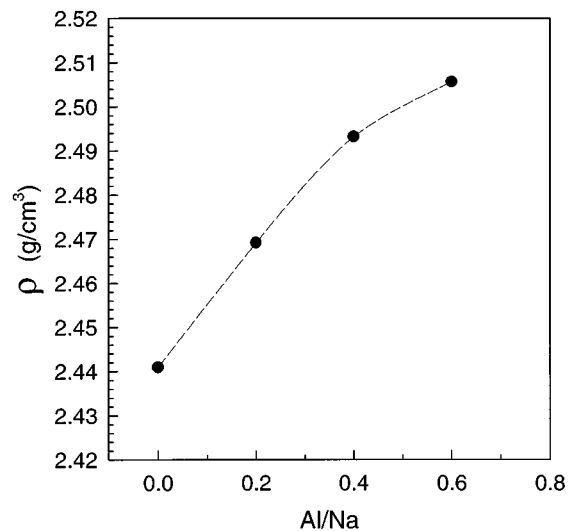


FIG. 5. Densities of the SAS glasses at room temperature.

IV. DISCUSSION

A. Chemical structure of SAS glasses

In the previous XPS study of the SAS glasses,¹² it was found from the analysis of O 1s spectra that aluminum ions form four coordinated tetrahedra at the expense of nonbridging oxygen ions. Since the aluminum tetrahedra, like the nonbridging oxygen ions, have a formal negative charge on them, some of the sodium ions which were associated with the nonbridging oxygen ions in the sodium trisilicate glass would become associated with the aluminum tetrahedra. From the increase of Na 1s binding energy, it was concluded that sodium ions are only partially ionized in the sodium trisilicate glass, and their ionicity increases with increasing amount of aluminum substitution. However, it was not clear at that time how the electrons donated by the sodium ions were distributed in the glass. We intend to answer this question in this article and present additional analysis of the chemical bonding and charge distribution in the SAS glasses.

To obtain a comprehensive picture of the chemical structure, it is important to first understand the distribution of Na 3s¹ valence electrons in the glasses. When sodium ions are associated with nonbridging oxygen ions, as shown in Fig. 6, the Na 3s¹ electrons participate with O 2p electrons in the formation of a bond between the two atoms. The nature of these bonds is only partially ionic,¹² i.e., the Na 3s¹ electrons are distributed between the nonbridging oxygen and the sodium ions. On the other hand, when sodium ions are associated with aluminum tetrahedra, the Na 3s¹ electrons are donated to the aluminum tetrahedra so that aluminum atoms may form tetrahedral bonds. The Na 3s¹ electrons are therefore more removed from sodium atoms in this case than in the previous case. Accordingly, it is expected that the sodium ions which are associated with aluminum tetrahedra should have a higher ionicity than those associated with nonbridging oxygen ions.

If it was possible to distinguish the sodium ions associated with two different kinds of charge-compensating centers in x-ray photoelectron spectra because of their charge density

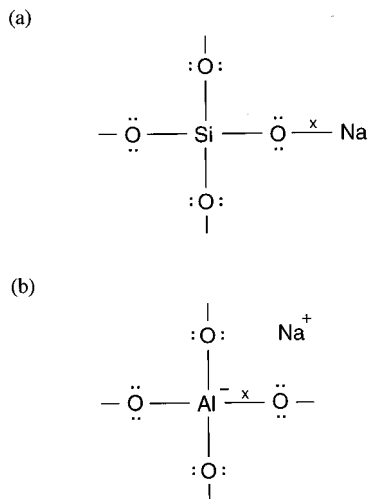


FIG. 6. Lewis electron-dot formulas of (a) a silicon tetrahedron with a nonbridging oxygen and a sodium ion; (b) an aluminum tetrahedron with a sodium ion. The Na $3s^1$ electrons are explicitly indicated by the mark x .

difference, one would expect two Na $1s$ peaks in the spectra: one with lower binding energy representing the sodium ions associated with nonbridging oxygen ions, and the other with higher binding energy representing the sodium ions associated with aluminum tetrahedra. Furthermore, the relative area ratio of the higher binding-energy peak to the lower one should increase to reflect the increasing aluminum substitution for silicon in the present SAS glass series. However, the experimental results show that there is only one Na $1s$ photoelectron peak which shifts to a higher binding-energy position with increasing aluminum substitution. This result indicates that as far as XPS can perceive sodium ions have only one well-defined average chemical state in the SAS glasses instead of having two distinct chemical states corresponding to its bonding with either nonbridging oxygen ions or aluminum tetrahedra.

In recent studies of the structure of sodium aluminosilicate glass by extended x-ray absorption fine structure (EXAFS)¹⁵ and molecular dynamic (MD) simulation,^{16,17} it is found that the oxygen coordination number of sodium ions is ~ 5 – 8 . This coordination number would include all of the three types of oxygen that can be distinguished by XPS, *viz.*, Si–O–Si (bridging oxygen), Si–O–Al (in aluminum tetrahedron), and Si–O–Na (nonbridging oxygen). A sodium ion is, therefore, charge compensated by nonbridging oxygen ions and aluminum tetrahedra at the same time rather than being associated with just one of them. This is illustrated schematically in Fig. 7(a) for a sodium ion surrounded by nonbridging oxygen ions (for charge compensation) and bridging oxygen atoms representing the sodium trisilicate glass; for the case of the SAS glasses, a sodium ion is shown in Fig. 7(b) to be surrounded by both nonbridging oxygen ions and aluminum tetrahedra for charge compensation, and bridging oxygen atoms. Furthermore, since the oxygen coordination number of sodium ion is high, it is reasonable to think that the sodium coordination number of nonbridging oxygen or aluminum tetrahedron is also more than one in the present SAS glasses. It is, therefore, not possible to identify

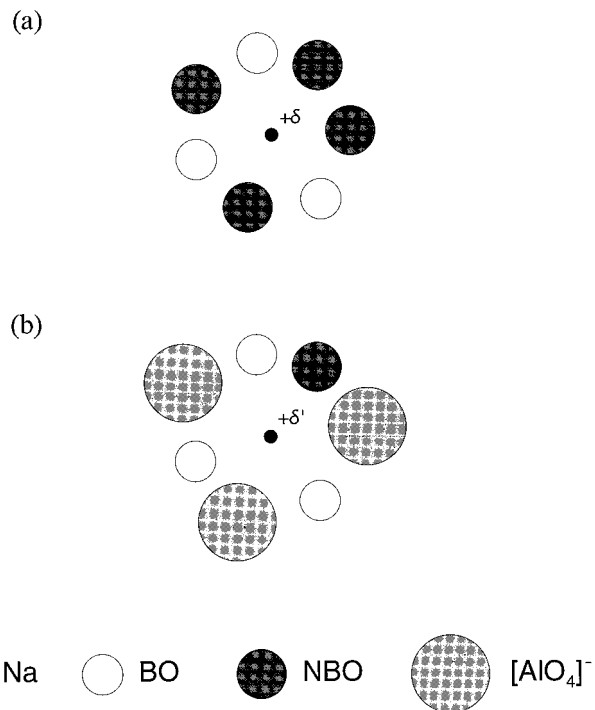


FIG. 7. Environment of a sodium ion consisting of: (a) bridging and nonbridging oxygen atoms in sodium trisilicate glass, and (b) bridging and nonbridging oxygen atoms as well as aluminum tetrahedra in SAS glass. δ and δ' are charges on sodium ions in respective glasses with $\delta' > \delta$.

which sodium ion donates its $3s^1$ electron to a particular nonbridging oxygen or aluminum tetrahedron. It appears more realistic that the sodium ions contribute electrons as a group, and the nonbridging oxygen and the aluminum tetrahedron take the electrons according to their need. Apparently, the electron need is greater for an aluminum tetrahedron than for a nonbridging oxygen. Accordingly the average electron density on each sodium ion decreases when more aluminum atoms substitute in the glass structure.

An important feature of the above model is that with varying aluminum substitution, there is no appreciable change in electron density around aluminum and the three types of oxygen ions; only the amounts of these species change. This is consistent with the XPS results that the binding energies of Al $2p$ and the three O $1s$ peaks do not vary significantly with composition.

In summary, sodium ions have a well-defined chemical state in the SAS glasses. They are only partially ionized in sodium trisilicate glass, and their ionicity increases when silicon is substituted by aluminum. A sodium ion is surrounded by a number of nonbridging oxygen ions and aluminum tetrahedra, and it is not possible to distinguish between the sodium ions which contribute the electron to a certain nonbridging oxygen ion or aluminum tetrahedron. The XPS binding energy of the inner electrons of silicon, aluminum, and oxygen ions remains essentially unchanged.

B. Dielectric constant of SAS glasses

Dielectric constant of a material originates from the electrical polarization of atoms, ion pairs, or molecular units at a

TABLE II. Analysis of the dielectric constant of the SAS glasses. $\epsilon_{i.f.}$ is the intermediate-frequency dielectric constant, ϵ_{∞} is the high-frequency dielectric constant, ρ is the density, V_m is the molar volume, P_m is the molar polarizability, α_t is the total molecular polarizability, α_j is the polarizability of the j th unit, where unit 1, 2, and 3 are $[\text{SiO}_2]$, $[\text{O}_{1/2}\text{-Na}]$, and $[\text{AlO}_2\text{-Na}]$, respectively. $\Delta\alpha_t$ is the difference of total molecular polarizability between a SAS glass and sodium trisilicate glass, and $\Delta\alpha_j$ is the polarizability difference between unit 3 and units 1 and 2. The superscripts e and i refer to the electronic and ionic contributions, respectively.

				Total polarizability				
Al/Na	$\epsilon_{i.f.}$	ρ (g/cm ³)	V_m (cm ³)	P_m (cm ³)	α_t (Å ³)	α_j (Å ³)	$\Delta\alpha_t$ (Å ³)	$\Delta\alpha_j$ (Å ³)
0	7.3	2.441	24.81	16.81	6.66	α_2 : 5.48
0.2	7.6	2.469	25.43	17.48	6.93	α_3 : 9.92	0.27	-0.79
0.4	8.0	2.493	26.17	18.32	7.26	α_3 : 10.09	0.60	-0.62
0.6	8.8	2.506	27.15	19.61	7.77	α_3 : 10.53	1.11	-0.18
Fused silica	3.8	2.20	27.31	13.18	5.23	α_1 : 5.23		
				Electronic polarizability				
Al/Na	ϵ_{∞}			P_m^e (cm ³)	α_t^e (Å ³)	α_j^e (Å ³)	$\Delta\alpha_t^e$ (Å ³)	$\Delta\alpha_j^e$ (Å ³)
0	2.236			7.24	2.87	α_2^e : 1.30
0.2	2.248			7.47	2.96	α_3^e : 3.70	0.09	-0.56
0.4	2.254			7.72	3.06	α_3^e : 3.68	0.19	-0.58
0.6	2.287			8.15	3.23	α_3^e : 3.85	0.36	-0.41
Fused silica	2.13			7.47	2.96	α_1^e : 2.96		
				Ionic polarizability				
Al/Na				P_m^i (cm ³)	α_t^i (Å ³)	α_j^i (Å ³)	$\Delta\alpha_t^i$ (Å ³)	$\Delta\alpha_j^i$ (Å ³)
0				9.57	3.79	α_2^i : 4.19
0.2				10.01	3.97	α_3^i : 6.22	0.18	-0.23
0.4				10.60	4.20	α_3^i : 6.41	0.41	-0.04
0.6				11.46	4.54	α_3^i : 6.68	0.75	0.23
Fused silica				5.71	2.26	α_1^i : 2.26		

microscopic level. Classical Clausius–Mossotti equation relates dielectric constant ϵ to the polarizability α of these structural units and their number density, N :

$$\frac{\epsilon - 1}{\epsilon + 2} = \frac{4\pi}{3} \sum_j N_j \alpha_j. \quad (1)$$

Equation (1) is in cgs units, and the summation is taken over various j structural units. The disordered nature of glass structure satisfies the assumption of local field used in deriving the Clausius–Mossotti equation. The number density N_j can be expressed as $N_j = N_0 N_{jm} / V_m$, where N_0 is the Avogadro's number, N_{jm} is the mole fraction of j th structural unit, and V_m is the molar volume. If the molar polarizability P_m is defined as¹⁸

$$P_m \equiv \frac{4\pi}{3} N_0 \sum_j N_{jm} \alpha_j \quad (2)$$

then the Clausius–Mossotti equation becomes

$$\frac{\epsilon - 1}{\epsilon + 2} = \frac{P_m}{V_m}. \quad (3)$$

The molar volume of the present SAS glasses was calculated using $V_m = M_m / \rho$ where M_m is the molar weight, and ρ is the

density; the molar polarizability was calculated from Eq. (3) using observed ϵ and V_m . The results of these calculations are reported in Table II.

The mechanisms of dielectric polarization responsible for $\epsilon_{i.f.}$ include both the electronic polarization and the ionic polarization. The molar polarizability is, therefore, a sum of the electronic molar polarizability P_m^e , and the ionic molar polarizability P_m^i i.e., $P_m = P_m^e + P_m^i$. The electronic molar polarizability can be calculated by the Clausius–Mossotti equivalent Lorentz–Lorenz equation for optical frequencies, by using optical frequency dielectric constant ϵ_{∞} which is related to the index of refraction n by the equation $\epsilon_{\infty} = n^2$. The ionic molar polarizability is, therefore, calculated by subtracting P_m^e from P_m . The indices of refraction of the SAS glasses are taken from Ref. 19 with $n = 1.495$, 1.499, 1.502, and 1.512 for $x = 0$, 0.2, 0.4, and 0.6 glasses, respectively. The calculated values of P_m^e and P_m^i are shown in Table II.

For the discussion of polarizabilities at microscopic level, it is convenient to define a total molecular polarizability per mole as $\alpha_t \equiv \sum N_{jm} \alpha_j$ which is then related to P_m by $P_m = (4\pi N_0 / 3) \alpha_t$. The variation trend of P_m and α_t is, therefore, the same because of the linear proportionality. Similarly, we define $P_m^e = (4\pi N_0 / 3) \alpha_t^e$ and $P_m^i = (4\pi N_0 / 3) \alpha_t^i$, where α_t^e and α_t^i are the electronic and

ionic molecular polarizability, respectively. Note that the polarizabilities are additive, i.e., $\alpha_i = \alpha_i^e + \alpha_i^i$. The calculated α_i 's, α_i^e 's, and α_i^i 's are also reported in Table II. The variation of the molar and the molecular polarizabilities with composition can be understood in terms of the variation of N_j 's and α_j 's as discussed next.

The microscopic sources of dielectric polarization in the present SAS glasses can be conveniently considered by dividing the structure of glass into three parts: the silicon tetrahedra [SiO₂], the nonbridging oxygen–sodium ion pairs [O_{1/2}–Na], and the aluminum tetrahedra–sodium ion units [AlO₂–Na]. The polarizabilities of these structural units are designated as α_1 for [SiO₂], α_2 for [O_{1/2}–Na], and α_3 for [AlO₂–Na]. According to the composition formula of the SAS glasses, there are 3–2*x* mol of [SiO₂], 2–2*x* mol of [O_{1/2}–Na], and 2*x* mol of [AlO₂–Na] per 4–*x* mole glass. Therefore,

$$\alpha_i = \sum_j N_{jm} \alpha_j = \frac{1}{4-x} [(3-2x)\alpha_1 + (2-2x)\alpha_2 + 2x\alpha_3]. \quad (4)$$

There are, thus, two structural variables (α_1 and α_2) for sodium trisilicate glass and three (α_1 , α_2 , and α_3) for the SAS glasses. Having only one experimentally obtained parameter α_i , it is not possible to determine α_j 's independently for each glass composition.

So to evaluate the α_j 's, an assumption is made that the polarizabilities of structural units remain constant with respect to composition. Then α_j 's are determined as follows: first, α_1 is calculated for fused silica since [SiO₂] is the only constituent structural unit; then, α_2 is calculated for sodium trisilicate glass by using the value of α_1 ; finally, α_3 is calculated for SAS glasses by using the values of α_1 and α_2 . It has been found that an error from using α_1 obtained for fused silica for analyzing α_2 for sodium trisilicate glass would only introduce a constant error in the absolute values of α_3 , but not in its relative values. Therefore, a variation of α_3 with composition would indicate the possible variations of true α_1 , α_2 , or α_3 with composition, and would verify the validity of our assumption that the polarizabilities of structural units in the SAS glasses are composition independent.

The electronic polarizabilities, α_j^e 's, and the ionic polarizabilities, α_j^i 's of the structural units can also be calculated by the same procedure as adopted above for the α_j 's. For the calculation of α_1 , $\epsilon_{i.f.} = 3.8$,²⁰ $\epsilon_{\infty} = 2.13$ ($n = 1.46$),²¹ and $\rho = 2.20$ g/cm³ (Ref. 21) are used for fused silica. The results of this calculation given in Table II show that the ionic polarizability of the structural units in the SAS glasses varies significantly with composition, but their electronic polarizability remains almost constant. Therefore, the overall polarizability has a significant composition dependence mainly because of the variation of ionic polarizability. The calculated electronic polarizabilities of the structural units are close to the true values; whereas, the calculated ionic and overall polarizabilities only indicate the qualitative trend of the true polarizabilities.

From the above evaluation of the polarizabilities of the structural units, the effect of the substitution of Al for Si on molecular polarizability can be readily understood. In this

TABLE III. Electronic polarizability of oxygen ions α_O^e , in various structural units.

Al/Na	α_O^e (Å ³)		
	Si–O–Si	Si–O–Al	Si–O–Na
0	1.48	...	2.59
0.2	1.48	1.85	2.59
0.4	1.48	1.84	2.59
0.6	1.48	1.92	2.59

regard, a polarizability difference, $\Delta\alpha_i$, is defined as the difference between α_i for the SAS and sodium trisilicate glasses. Also, a polarizability difference of [AlO₂–Na] and [SiO₂]+[O_{1/2}–Na] structural units is termed as $\Delta\alpha_j = \alpha_3 - (\alpha_1 + \alpha_2)$. It can be deduced from Eq. (4) that $\Delta\alpha_i = 2x\Delta\alpha_j$. Therefore, the variation of α_i with *x* depends on the polarizability difference between [AlO₂–Na] and [SiO₂]+[O_{1/2}–Na] as well as the extent of aluminum substitution. The calculated values of $\Delta\alpha_i$ and $\Delta\alpha_j$ are shown in Table II. It can be seen that the substitution of Al for Si in the SAS glasses results in a smaller electronic polarizability of [AlO₂–Na] than that of [SiO₂]+[O_{1/2}–Na]. The effect of this substitution on the ionic polarizability is, however, unclear because of the qualitative nature of the calculated α_j^i 's.

C. Correlation between dielectric constant and chemical structure

1. Electronic polarizability

The electronic polarization arises from the shift of the center of the negative electron cloud in relation to the positive atom nucleus in an electric field. In the simplest case of a monatomic gas, the electronic polarizability of an atom is proportional to the volume of the atom. In solids also, the electronic polarizability generally increases with the size of the ion, but the dependence on composition is considerably more complicated by the redistribution of charge during bonding. In general, the density of electron charge is relatively more important for a negative ion since its outer electrons are less firmly bound than those of a positive one. Among the four ions, (O, Na, Al, and Si), in SAS glasses, oxygen being an anion has the largest electronic polarizability.^{22,23} In fact, its electronic polarizability is so much larger that, by comparison, the polarizability of the other three elements may be neglected. Therefore, we discuss the calculated electronic polarizability of the SAS glasses in terms of the polarizability of oxygen ions only.

As noted in the previous section, the electronic polarizability of the various structural units in SAS glasses remains essentially constant. It is, then, possible to calculate the electronic polarizability of the oxygen ions α_O^e by dividing the electronic polarizability of various units by the number of oxygen ions in each unit, *viz*: two oxygen atoms with Si–O–Si bond in a [SiO₂] unit; two oxygen atoms with Si–O–Al bond in a [AlO₂–Na] unit; and one half of an oxygen ion with Si–O–Na bond in a [O_{1/2}–Na] unit. The result of the calculation is shown in Table III. The polarizability for oxygen ions in Si–O–Si and Si–O–Na bonds is

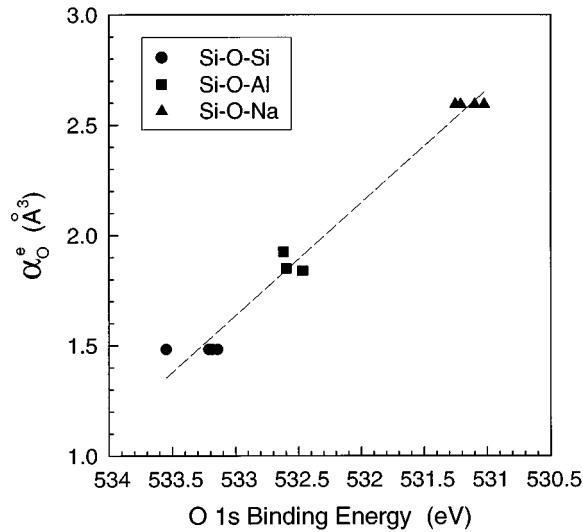


FIG. 8. Correlation between the electronic polarizability of oxygen ions and the O 1s XPS binding energy in the SAS glasses.

independent of composition as assumed. All the possible variation of the electronic polarizability of oxygen ions is reflected in a small change of the polarizability of oxygen ions in Si–O–Al. Nevertheless, there is a significant difference among the values for different units, specifically the electronic polarizability of oxygen ions increases in the order of Si–O–Si < Si–O–Al < Si–O–Na.

Next we examine the relationship between polarizability and electron charge density around oxygen. According to Fig. 8, we find a simple correlation between the electronic polarizability of different types of oxygen ions and the O 1s XPS binding energy plotted on a decreasing binding energy scale. A good linear relationship between the two parameters is given by the dashed straight line which is obtained by linear regression of all the data points in the plot. It was previously shown¹² that the degree of negative charge on oxygen ions is inversely proportional to the O 1s binding energy. Therefore, as the O 1s binding energy decreases from Si–O–Si to Si–O–Na, the degree of negative charge on oxygen ions increases. Consequently, Fig. 8 implies that the electronic polarizability of oxygen ions increases linearly with the degree of negative charge on the ions in the SAS glasses. We believe this is the first demonstration of a simple relationship between the electronic polarizability and an experimentally obtained charge density parameter.

2. Ionic polarizability

The ionic polarization arises from the displacement of positive and negative ions in relation to one another in an electric field. The ionic polarizability α_i of ion pairs can be described by the oscillator model as:

$$\alpha^i = \frac{z^2 e^2}{(2\pi\nu_0)^2 m}, \quad (5)$$

where ze is the charge on an ion, ν_0 is the lattice vibration frequency, and m is the reduced mass.^{24,25} The denominator of Eq. (5) is simply the force constant of the bond between

TABLE IV. Ionic polarizability of sodium ions: α_{Na}^i as calculated from dielectric measurements, and α_{Na}^{i*} as determined theoretically assuming complete ionization of sodium ions. ν_{eff} is the effective vibration frequency of sodium ions.

Al/Na	α_{Na}^i (\AA^3)	ν_{eff} (cm^{-1})	α_{Na}^{i*} (\AA^3)	$(\alpha_{\text{Na}}^i/\alpha_{\text{Na}}^{i*})^{1/2}$
0	4.14	173	5.68	0.854
0.2	4.56	168	6.02	0.870
0.4	5.05	165	6.24	0.899
0.6	5.67	156	6.98	0.901

the ions. Clearly, the ionic polarizability is strongly affected by the chemical structure of the ions. The ionic polarizability of individual molecular units is more complicated to quantify, but it should depend on the bonding in a similar way. In SAS glasses, the ionic polarizability should include contribution from the vibrations within silicon and aluminum tetrahedra, and the vibration of sodium ions with respect to their charge compensating surroundings consisting of nonbridging oxygen ions and aluminum tetrahedra.

From the analysis of dielectric constant in Sec. IV B, the ionic polarizability of the structural units in SAS glasses is found varying significantly with composition. Since the silicon, aluminum, and oxygen XPS peak positions remain almost unchanged (see Sec. III A), the ionic polarizability of $[\text{SiO}_2]$ and $[\text{AlO}_2]$ units is assumed to be constant. The variation of ionic polarizability with composition is, therefore, attributed to the change of polarizability of sodium ions with respect to their surroundings. Furthermore, since a sodium ion is surrounded by a cage of several nonbridging oxygen ions and aluminum tetrahedra, and it has a well-defined chemical state, its vibrations with respect to surroundings can be considered as those of an oscillator made up of the sodium ion itself and the charge center of its cage. In this description, the ionic polarizability of sodium ions α_{Na}^i can be considered as an average of $[\text{O}_{1/2}\text{-Na}]$ and $[\text{AlO}_2\text{-Na}]$ bonds according to their relative concentration. That is, $\alpha_{\text{Na}}^i = [(2-2x)\alpha_2^i + 2x\alpha_3^i]/[(2-2x) + 2x] = (1-x)\alpha_2^i + x\alpha_3^i$ according to Eq. (4). One should note that the ionic polarizability of aluminum tetrahedra is inherently included in α_3^i . It is not a part of the vibrations of sodium ions and is assumed to be constant. The calculated values of α_{Na}^i are reported in Table IV which shows that the ionic polarizability of sodium ions increases with increasing concentration of aluminum in the SAS glasses.

If the description of vibration involving sodium ions is simplified by considering it as an oscillator, the ionic polarizability of sodium ions can be calculated from Eq. (5). In this calculation, ν_0 is taken as the effective vibration frequency of sodium ions, ν_{eff} , obtained from far-infrared spectra of the present glasses.^{26,27} The m is taken to be the mass of a sodium ion since the mass of the *site* is considerably larger than that of a sodium ion. A directly measured value of z is not available from experiments, so a value of $z=1$ is used assuming a total ionic character of sodium ions. The sodium ionic polarizability thus calculated is designated as α_{Na}^{i*} with a superscript * to indicate assumed complete ionization of sodium with $z=1$. The results of ν_{eff} and α_{Na}^{i*} are shown in Table IV. Since α_{Na}^i , which is obtained from the

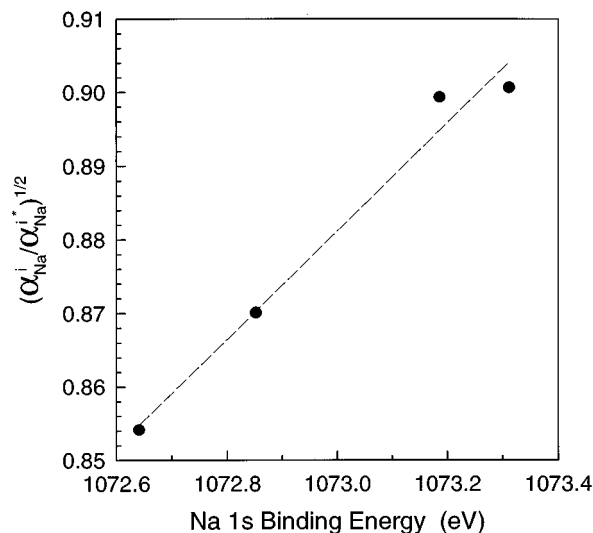


FIG. 9. Correlation between the ionic polarizability of sodium ions and the Na 1s XPS binding energy in the SAS glasses.

dielectric constant analysis, contains possible deviation of z from 1 because of the partially ionic characteristics of sodium ions, the square root of the ratio of experimental α_{Na}^i to theoretical α_{Na}^{i*} should be proportional to the actual value of z . Table IV shows that this ratio, $(\alpha_{\text{Na}}^i / \alpha_{\text{Na}}^{i*})^{1/2}$, increases with increasing aluminum amount in the SAS glasses.

To establish a relation between ionic polarizability and the chemical structure of glass, $(\alpha_{\text{Na}}^i / \alpha_{\text{Na}}^{i*})^{1/2}$ is plotted against the Na 1s XPS binding energy in Fig. 9. It shows that $(\alpha_{\text{Na}}^i / \alpha_{\text{Na}}^{i*})^{1/2}$ increases linearly with Na 1s binding energy. Since an increase of Na 1s binding energy implies an increase of the positive charge on sodium ions, Fig. 9 suggests a parabolic dependence of α_{Na}^i on the actual charge z and reveals the importance of the experimentally determined chemical structure for determining the ionic polarizability.

V. CONCLUSIONS

Sodium ions have a well-defined chemical state in SAS glasses. They are only partially ionized in sodium trisilicate glass, and their ionicity increases when silicon is substituted by aluminum. A sodium ion is surrounded by several non-bridging oxygen ions and aluminum tetrahedra, and it is not possible to identify which sodium ion contributes the electron to a certain nonbridging oxygen ion or aluminum tetrahedron. The ionicity of silicon, aluminum, and oxygen atoms remains essentially unchanged in these SAS glasses.

The dielectric constant of the SAS glasses increases with increasing Al substitution. The electronic polarizability of constituent structural units remains constant with composition, while their ionic polarizability increases with increasing aluminum substitution.

The electronic polarizability of oxygen ions increases in the order of Si–O–Si < Si–O–Al < Si–O–Na. It depends linearly on the negative charge on oxygen ions, and can be correlated to the O 1s XPS binding energy. The ionic polarizability of sodium ions increases with increasing amount of aluminum in the SAS glasses. It correlates directly with the Na 1s XPS binding energy.

ACKNOWLEDGMENTS

The authors wish to thank Dr. A. C. Miller for his help with the XPS experiments, and the National Science Foundation for financial support under Grant No. DMR-9225072. A grant from NATO (No. CRG931213) for international collaboration is also gratefully acknowledged.

- ¹G. Geiger, *Ceram. Bull.* **69**, 1131 (1990).
- ²R. R. Tummala, *J. Am. Ceram. Soc.* **74**, 895 (1991).
- ³K. Kobayashi, *J. Non-Cryst. Solids* **109**, 277 (1989).
- ⁴P. W. Bless, R. L. Wahlers, and S. J. Stein, in *Glasses for Electronic Applications*, edited by K. M. Nair (The American Ceramic Society, Westerville, OH, 1991), p. 397.
- ⁵G. M. Singer and M. Tomozawa, *Phys. Chem. Glasses* **30**, 86 (1989).
- ⁶P. N. Kumta and M. A. Sriram, *J. Mater. Sci. A* **28**, 1097 (1993).
- ⁷S. C. Cherukuri and S. K. Dey, in *Glasses for Electronic Applications*, edited by K. M. Nair (The American Ceramic Society, Westerville, OH, 1991), p. 355.
- ⁸S. V. J. Kenmuir, J. S. Thorp, and B. L. J. Kulesza, *J. Mater. Sci.* **18**, 1725 (1983).
- ⁹R. N. Hampton, W. Hong, G. A. Saunders, and R. A. El-Mallawany, *Phys. Chem. Glasses* **29**, 100 (1988).
- ¹⁰R. El-Mallawany, *Mater. Chem. Phys.* **37**, 376 (1994).
- ¹¹H. A. A. Sidek, I. T. Collier, R. N. Hampton, G. A. Saunders, and B. Bridge, *Philos. Mag. B* **59**, 221 (1989).
- ¹²C. H. Hsieh, H. Jain, A. C. Miller, and E. I. Kamitsos, *J. Non-Cryst. Solids* **168**, 247 (1994).
- ¹³A. K. Jonscher, *Nature* **267**, 673 (1977).
- ¹⁴C. H. Hsieh and H. Jain, *J. Non-Cryst. Solids* **183**, 1 (1995).
- ¹⁵D. A. McKeown, G. A. Waychunas, and G. E. Brown, Jr., *J. Non-Cryst. Solids* **74**, 325 (1985).
- ¹⁶D. M. Zirl and S. H. Garofalini, *J. Am. Ceram. Soc.* **73**, 2848 (1990).
- ¹⁷Y. Cao and A. N. Cormack, in *Diffusion in Amorphous Materials*, edited by H. Jain and D. Gupta (The Minerals, Metals & Materials Society, Warrendale, PA, 1994), p. 137.
- ¹⁸W. D. Kingery, H. K. Bowen, and D. R. Uhlmann, *Introduction to Ceramics*, 2nd ed. (Wiley, New York, 1976), Chap. 18.
- ¹⁹J. Schroeder, *J. Non-Cryst. Solids* **40**, 549 (1980).
- ²⁰R. N. Hampton, I. T. Collier, H. A. A. Sidek, and G. A. Saunders, *J. Non-Cryst. Solids* **110**, 213 (1989).
- ²¹N. P. Bansal and R. H. Doremus, *Handbook of Glass Properties* (Academic, Orlando, FL, 1986), Chap. 2.
- ²²C. Kittel, *Introduction to Solid State Physics*, 6th ed. (Wiley, Singapore, 1986), Chap. 13.
- ²³H. Rawson, *Properties and Applications of Glass* (Elsevier, Amsterdam, The Netherlands, 1980), Chap. 6.
- ²⁴G. G. Agrawal, H. P. Sharma, and J. Shanker, *J. Phys. Chem. Solids* **38**, 815 (1977).
- ²⁵A. K. Varshneya, *Fundamentals of Inorganic Glasses* (Academic, San Diego, CA 1994), Chap. 19.
- ²⁶E. I. Kamitsos, J. A. Kapoutsis, H. Jain, and C. H. Hsieh, *J. Non-Cryst. Solids* **171**, 31 (1994).
- ²⁷E. I. Kamitsos, J. A. Kapoutsis, H. Jain, and C. H. Hsieh (to be published).